Timber Defect Identification: Enhanced Classification with Residual Networks

Teo Hong Chun[1], Ummi Raba'ah Hashim[2], Sabrina Ahmad[3]
Centre for Advanced Computing Technology, Fakulti Teknologi Maklumat dan Komunikasi (FTMK), Universiti Teknikal Malaysia Melaka (UTeM), Malaysia[1, 2, 3]
Department of Information Technology and Communication, Politeknik Ungku Omar, Perak, Malaysia[1]

***Abstract*—This study investigates the potential enhancement of classification accuracy in timber defect identification through the utilization of deep learning, specifically residual networks. By exploring the refinement of these networks via increased depth and multi-level feature incorporation, the goal is to develop a framework capable of distinguishing various defect classes. A sequence of ablation experiments was conducted, comparing our proposed framework's performance (R1, R2 and R3) with the original ResNet50 architecture. Furthermore, the framework's classification accuracy was evaluated across different timber species and statistical analyses such as independent t-tests and one-way ANOVA tests were conducted to identify the significant differences. Results showed that while the R1 architecture demonstrated slight improvement over ResNet50, particularly with the addition of an extra layer ("ConvG"), the latter still maintained superior overall performance in defect identification. Similarly, the R2 architecture, despite achieving notable accuracy improvements, slightly lagged behind R1. Integration of fully pre-activation activation functions in the R3 architecture yielded significant enhancements, with a 14.18% increase in classification accuracy compared to ResNet50. The R3 architecture showcased commendable defect identification performance across various timber species, though with slightly lower accuracy in Rubberwood. Nonetheless, its performance surpassed both ResNet50 and other proposed architectures, suggesting its suitability for timber defect identification. Statistical analysis confirmed the superiority of the R3 architecture across multiple timber species and this underscores the significance of integrating network depth and fully pre-activation activation functions in improving classification performance. In conclusion, while the wood industry has made strides towards automation in timber grading, significant challenges remain. Overcoming these challenges will require innovative approaches and advancements in image processing and artificial intelligence to realize the full potential of automated grading systems.**

Keywords*—*Residual neural network; convolutional neural network; timber defect identification; deep learning

I. INTRODUCTION

Timber grading and defect identification are important in wood industries as it serve as cornerstone for the decision made by operators. In the past, these tasks were executed manually requiring careful assessment of the timber to determine their quality and economic value. This procedure involved classifying each log relative to their grade by assessing a number of factors such as geometry and typed of defect presence. Nevertheless, manual grading methods are often prone to subjectivity, time consumption, and human error [1]. In light of current state of the industry, a notable concern arises regarding the consistent or potentially declining number of qualified inspectors in comparison to the steadily growing market [2]. Additionally, timber grading process would usually involve a complex classification procedure such as sorting by defects, species and texture which require a versatile algorithm that are capable of handling diverse tasks on the same machine. Moreover, timber defects that resulted from environment and natural growth processes might have an impact on the timber strength, durability and aesthetic appeal, thereby affecting its economic value. The current methods of timber defect detection rely heavily on visual inspection which is subjective and lack of precision, to overcome these challenges.

In recent years, there has been a rise in quality control using automated vision inspection (AVI) among the manufacturer, particularly in the secondary timber industry with the objective to overcome present issues [3]. Although AVI has been applied in the timber industry to address these challenges, ongoing research endeavors persist in enhancing the inspection process across various domains, including defect detection and identification, characterizing defect, grading timber, and integrating sensors into hardware components for optimizing cutting processes [4]. A number of methods have been proposed [5][6][7][8][9] to streamline the grading process, yet they still encounter several obstacles especially in the scope of detection and identification of timber defects. To address these challenges, there is a growing interest in leveraging statistical classifier methods such as machine learning and deep learning algorithms in AVI for the identification of timber defects as these technologies offer the potential expedited, reproducible and reliable grading processes [10][11][12][13]. A 2020 study suggests that employing deep learning for automated feature extraction could yield higher precision while enhancing accuracy by at least 4% compared to other timber feature extraction and recognition methods [14]. In [15], they employed a DenseNet network along with a single-shot multi-box detector (SSD) and a target detection algorithm to develop an enhanced SSD algorithm for detecting defects in solid wood panels. Despite facing challenges in accurately identifying active knots due to their similarity to background features, the proposed method achieved an improved accuracy rate of 96.1% compared to earlier version. However, such autonomy come with the trade-off where it requires a significantly greater amount of data to train the deep learning architecture compared to the machine learning approaches. As deep learning advances swiftly,

numerous Convolutional Neural Network (CNN) architectures have surfaced over time to address issues across various domains of defect identification such as AlexNet [16], MobileNetV2 [17], GoogLeNet [18] and ResNet [19]. In this research, our emphasis will be on employing Residual Neural Network (ResNet) as our deep learning network architecture given its notable achievements in numerous image classification tasks in recent years [20].

He et al. [21] introduced the Residual Neural Network (ResNet), a Convolutional Neural Network (CNN) architecture inspired by the structure of pyramidal cells in the cerebral cortex. ResNet key innovation was residual learning, enabling more efficient training of deep networks through skip connections that bypass multiple layers while incorporating ReLU and batch normalization [21]. Additionally, there exist model such as HighwayNets that further facilitate training deep networks by using an additional weight matrix to learn skip weights [22]. The fundamental unit of the ResNet network is the residual building block, which constitutes the majority of its architecture. These blocks incorporate skip connections to bypass convolutional layers, mitigating issues such as gradient disappearance or explosion with increasing network depth [19]. Comprised of convolutional layers, batch normalizations, ReLU activation functions, and skip connections, the residual building block forms the backbone of ResNet's structure. Although augmenting the depth of a neural network enhances its feature extraction capabilities as highlighted by [23], however, adding more layers to a current deep model such as ResNet also lead to higher training error [21]. To tackle the issue of vanishing gradient, [22] proposed skip connections within residual neural networks where these connections diminish the shortest path from lower layer parameters to the output, mitigating the vanishing gradient problem. Furthermore, by employing fewer layers during the initial training phase, this skipping strategy simplifies the network architecture effectively. Fig. 1 illustrates the layout of fundamental residual block. The output of the residual building block can be expressed using Eq. (1), where F represents the residual function, and x and y denote the input and output of the residual function, respectively.

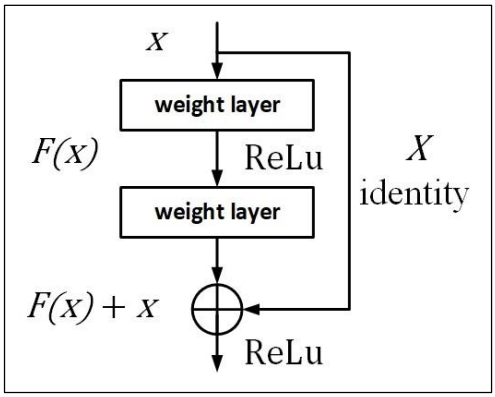

Fig. 1. Basic residual block.

$$y = F(x) + x \quad (1)$$

ResNet stands out for its significantly deeper network compared to its competitors, yet it maintains fewer parameters (weights) than other models. A comparative analysis of ResNet50 and other CNN architectures for timber species identification by Oktaria et al. [24] in 2019, demonstrated that residual network outperforms its counterparts in terms of F1 Score, precision, and accuracy. Similarly, [25] proposed a transfer learning approach using the ResNet50 architecture for plant disease identification, achieving a remarkable training accuracy of 99.80%. On the contrary, Ahmed et al. [26] utilized ResNet50 for the purposes of crack detection by training the model with dataset of 48000 images and achieve remarkable accuracy rate of 99.8%. Inspired by the aforementioned factors, we expanded our research on using residual neural network (ResNet) for identifying defects in Malaysian timber species, aiming for outcomes that could prove advantageous to the local timber product industries.

II. METHODOLOGY

A. Overview of Approach

Driven by the significance of network depth where deep convolutional neural networks have achieved remarkable progress in image classification [27] as well as the significant achievement of Resnet50 from studies related to identification of timber defects [28]. Therefore, we investigate the potential of enhancing better class representation thus achieving higher accuracy by employing a residual network as the base architecture for this study. Hence, our goal is to explore the refinement of residual network layer by incorporating multi-level features that can be enhanced through increased the number of stacked layer (depth). This study conducted a sequence of ablation experiments based on residual network architecture that were implemented to facilitate the development of timber defect identification framework with ability to distinguish different type of defect classes. Additionally, we compared the performance of our timber defect identification frameworks to the original ResNet50, which is based on the concept of residual networks. Furthermore, we evaluated the classification performance of our proposed timber defect identification framework across various timber species. Finally, we expanded the validation of our defect identification approach by conducting statistical analyses which include independent t-tests and one-way ANOVA tests to identify significant differences.

B. Residual Neural Network (ResNet) Architecture

Recent studies in timber defect identification have seen the development of several architectures based on the Residual Neural Network (ResNet) design, renowned for its efficiency in depth-based CNN architecture [29][30][31][32]. This research involves reformulating the layers of the residual network specifically for classification of timber defects by altering the residual block based on ResNet50 architecture as shown in Fig. 2. The ResNet50 architecture is a cutting-edge convolutional network comprising 50 layers, featuring skip connections. These skip connections which operate in parallel with standard convolutional layers, serve as shortcuts to aid the network in capturing global features while addressing the challenge of vanishing gradients encountered in deeper network layers [33]. Besides, the architecture is made up of 7x7 convolutional layer with 65 kernels, succeeded by a 3x4 max-pooling layer with a stride of 2, followed by 16 residual

building blocks, 7x7 average-pooling layer with a stride of 7, and a fully connected layer preceding the softmax output layer [25]. The inclusion of residual blocks helps diminishing the output size while simultaneously increasing the network's depth.

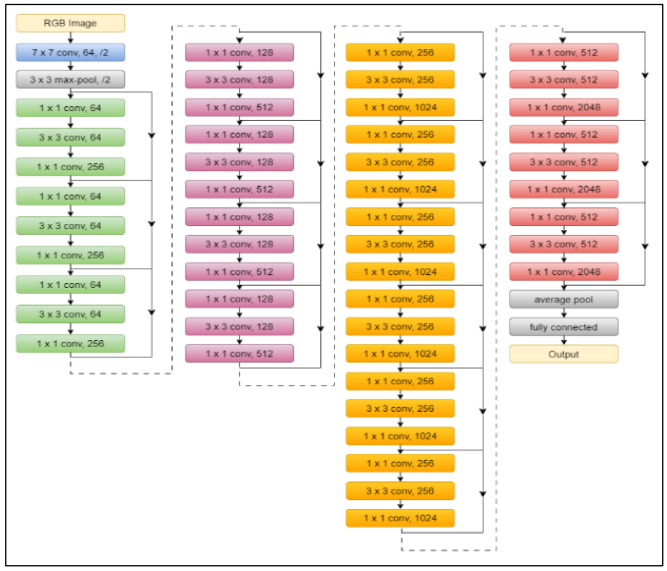

Fig. 2. ResNet50 architecture.

In this research, we systematically formulated three variations of residual network architecture with each employing different number and sizes of convolutional layers. This iterative approach was undertaken to explore the most appropriate configuration for timber defect identification framework. The experiment is performed on three proposed residual network architectures referred to as R1, R2, and R3. These variants draw inspiration from the architecture of ResNet50 as well as earlier research conducted by [21] in the field of deep residual learning. Each of the three devised versions of the residual network possesses its own unique architecture where R1 comprises 51 parameter layers, while the other variants exhibit a greater number of parameter layers, with R2 featuring 53 layers and R3 consisting of 54 layers. Additionally, within the architecture of both R1 and R2, we integrated "ConvG" and "ConvC+1" layers by introducing additional new residual blocks containing convolutional networks of different sizes into the proposed architectures. Table I illustrate the line-up of formulated residual network architectures employed for performance evaluation in this study.

TABLE I. FORMULATED RESIDUAL NETWORK ARCHITECTURE

Layer	Output Size	R1	R2	R3
ConvA	112x112	7x7, 64, stride 2		
ConvB	56x56	3x3 max pool, stride 2		
ConvC+1	56x56		$\begin{bmatrix} 1x1,32 \\ 3x3,32 \\ 1x1,128 \end{bmatrix} x3$	
ConvC	56x56	$\begin{bmatrix} 1x1,64 \\ 3x3,64 \\ 1x1,256 \end{bmatrix} x3$	$\begin{bmatrix} 1x1,64 \\ 3x3,64 \\ 1x1,256 \end{bmatrix} x3$	$\begin{bmatrix} 1x1,64 \\ 3x3,64 \\ 1x1,256 \end{bmatrix} x5$
ConvD	28x28	$\begin{bmatrix} 1x1,128 \\ 3x3,128 \\ 1x1,512 \end{bmatrix} x4$	$\begin{bmatrix} 1x1,128 \\ 3x3,128 \\ 1x1,512 \end{bmatrix} x4$	$\begin{bmatrix} 1x1,128 \\ 3x3,128 \\ 1x1,512 \end{bmatrix} x6$
ConvE	14x14	$\begin{bmatrix} 1x1,256 \\ 3x3,256 \\ 1x1,1024 \end{bmatrix} x6$	$\begin{bmatrix} 1x1,256 \\ 3x3,256 \\ 1x1,1024 \end{bmatrix} x6$	$\begin{bmatrix} 1x1,256 \\ 3x3,256 \\ 1x1,1024 \end{bmatrix} x6$
ConvF	7x7	$\begin{bmatrix} 1x1,512 \\ 3x3,512 \\ 1x1,2048 \end{bmatrix} x3$	$\begin{bmatrix} 1x1,512 \\ 3x3,512 \\ 1x1,2048 \end{bmatrix} x3$	$\begin{bmatrix} 1x1,512 \\ 3x3,512 \\ 1x1,2048 \end{bmatrix} x3$
ConvG	4x4	$\begin{bmatrix} 1x1,1024 \\ 3x3,1024 \\ 1x1,4096 \end{bmatrix} x1$		
	1x1	Average Pool, Fc, Softmax		

In addition to utilizing the original residual block, we investigated a revised version of the residual network architecture by integrating fully pre-activation activation functions in R3 where both Batch Normalization (BN) and Rectified Linear Unit (ReLU) layers precede the weight layer as illustrated in Fig. 3(b). The approach was introduced by He et al. [34] as a departure from the traditional "post-activation" paradigm which lead to a new residual block design that is easier to train and demonstrated enhanced generalization capabilities compared to the original ResNet architecture. Fig. 3(a) depicts the original ResNet residual block, where BN is applied after each weight layer, and ReLU is impemented after BN with the exception of the final ReLU within a Residual Unit which occurs after the element-wise addition. In reformulating the residual block for the R3 architecture, we implemented an asymmetric structure described by [34] which allow the new after-addition activation becomes an identity mapping. This new asymmetric form can be represented by the following equation:

$$X_{l+1} = X_l + F\left(\hat{f}(X_l), W_l\right),. \quad (2)$$

The design of the revised residual block allows for the adoption of a new after-addition activation $\hat{f}$ in an asymmetrical manner, effectively treating $\hat{f}$ as the pre-activation of the subsequent residual block.

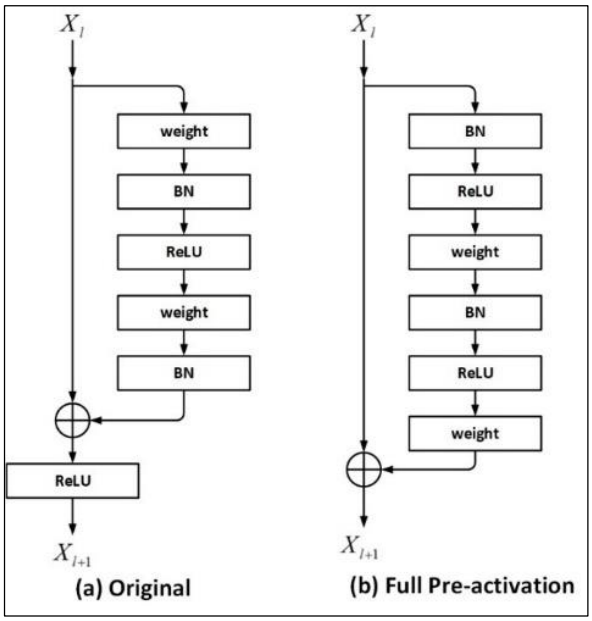

Fig. 3. ResNet50 residual block (a) Original (b) Full pre-activation.

C. Hyperparameter Optimization

To ensure the optimal performance of the three proposed residual network architecture, we conducted a further assessment of the appropriate CNN hyperparameter configuration focusing on both learning rate and epochs. The proposed architectures were trained using SGD optimizer with learning rate set at 0.001 and 0.0001. Throughout this experiment, the maximum number of epochs ranged from 50 to 200, with variations of 50, 100, and 200. The models underwent training on timber defect dataset encompassing various timber species (Meranti, Merbau, KSK, and Rubberwood) sourced from Universiti Teknikal Melaka Malaysia (UTeM) [35]. The experimental samples were then generated using 1600 augmented images of timber defect, comprises of eight timber defect categories (brown stain, blue stain, knot, borer holes, rot, bark pocket, wane, and split), as well as a set of clear timber specimens. The performance classification of each proposed architecture was assessed and compared with the transfer learning ResNet50 model to determine the most effective framework for identifying timber defects.

III. Result and Discussion

In this section, we will present the experimental outcomes of the three formulated residual network architectures to evaluate the efficacy of the proposed approaches in term of their performance in identification. The results are illustrated across three dimensions throughout the proposed residual network architecture where the first dimension explores different hyperparameter configurations encompassing both learning rate and epochs in pursuit of achieving highest classification performance for the proposed architecture (R1, R2, R3). Subsequently, a comparison of performance is conducted between the standard ResNet50 and the proposed architectures, with the goal of evaluating their classification performance in terms of improved representation of the defect class and accuracy. Finally, the identification performance is summarized across various timber species to gauge the consistency of performance of the proposed approach across multiple timber species. The experimental result for all three formulated architectures (R1, R2 and R3) across the timber species are presented in Table II with highest classification performance achieved using specific hyperparameter settings are highlighted in red. The data presented in Table II clearly indicates that the R1 architecture demonstrates commendable classification performance across all timber species datasets, achieving the highest identification accuracy for each species within the range of 89.85% to 94.44%. In R1, the Rubberwood dataset attains the highest classification accuracy of 94.44% with hyperparameter settings of 0.001 learning rate and 100 epochs. Following this, R1 achieves the second-highest classification performance reaching 93.48% in the Meranti dataset. Subsequently, KSK follows with an accuracy of 92.52%, and finally, the Merbau dataset records the lowest accuracy of 89.85%. On the contrary, the R2 architecture achieves the highest classification accuracy of 94.07% across all timber species with optimized hyperparameters (LR = 0.001, Epoch = 100) in rubber timber species. It was succeeded by Meranti (93.04%), Merbau (92.74%), and KSK (91.93%). It's noteworthy that the R2 highest classification accuracy across the timber species is achieved with a learning rate of 0.001, coupled with varying numbers of epochs: 100 for Rubberwood, 200 for Meranti, and 50 for both Merbau and KSK. By incorporating fully pre-activation functions into the R3 residual block, we achieved the highest classification performance of 99.11% in the Merbau dataset, utilizing a learning rate of 0.0001 and 200 epochs as the training hyperparameter settings. In the case of the remaining three timber species, the classification performance of R3 was as follows: Meranti (97.7%) with LR = 0.001 and Epoch = 100, KSK (98.59%) with LR = 0.0001 and Epoch = 200, and Rubberwood (96.59%) with LR = 0.001 and Epoch = 50.

As depicted in Fig. 4, the classification accuracy of the R1 architecture demonstrates a roughly 0.7% improvement compared to the original ResNet50 under different hyperparameter configurations across timber species. The improvement in performance stems from integrating an additional layer, denoted as "ConvG," into the network architecture of R1. Nonetheless, despite the noted rise in classification accuracy for R1 in contrast to ResNet50, the ResNet50 architecture still predominantly leads in overall performance concerning defect identification where highest classification accuracy achieved by R1 still falls short when compared to ResNet50 architecture. Similar to earlier R1 architecture, we evaluated the classification performance of the R2 architecture alongside the original ResNet50. The findings indicate that with 100 epochs and a learning rate of 0.001, the R2 architecture surpassed the original ResNet50 in the Merbau dataset, achieving an accuracy improvement of 6.92%. This implies that increasing the depth of the CNN architecture does enhance its classification accuracy. However, in comparison to R1, despite the inclusion of a new residual block ("ConvC+1")

with smaller convolutional layer sizes in the proposed architecture of R2, it was noted that R2's highest classification performance still slightly lags behind R1 by a marginal difference of 0.37%. Nevertheless, despite some improvement in classification performance, the ResNet50 architecture continues to dominate the overall performance in defect identification. Within the R3 architecture, we delve into fully pre-activation activation functions by incorporating both BN and ReLu layers prior to the weights in addition to the depth of CNN network architecture. Illustrated in Fig. 4., the proposed R3 architecture, integrated with both network depth and fully pre-activation activation functions does improves the architecture's classification performance in the Merbau species by 14.18% compared to the original ResNet50 while using a learning rate of 0.001 and 50 epochs. The performance of the R3 architecture is clearly commendable across different timber species, attaining defect identification accuracies ranging from 96.59% to 99.11%. Although it appears that the R3 architecture still exhibits lower performance in the Rubberwood species with a defect identification accuracy of 96.59% which marking the lowest R3 classification performance among the timber species. However, it's notable that the performance of the proposed R3 architecture has not only shown significant improvement across timber species and on average but has also outperform the classification performance of original ResNet50 and other proposed architectures (R1 and R2). This suggests that integrating both network depth and fully pre-activation activation functions into the R3 architecture improves the CNN's classification performance in distinguishing classes of timber defects and making it well-suited for implementation as our timber defect identification framework.

TABLE II. CLASSIFICATION PERFORMANCE OF R1, R2, R3 AND RESNET50 ACROSS TIMBER SPECIES USING MULTIPLE HYPERPARAMETERS SETTINGS. THE HIGHEST CLASSIFICATION ACCURACY ACROSS TIMBER SPECIES ARE HIGHLIGHTED IN RED

Architectures	Hyperparameters		Rubberwood	Merbau	Meranti	KSK
	Learning rate	Epoch				
R1	0.001	50	94.15	83.41	92.15	88.89
		100	94.44	87.19	90.96	92.3
		200	94.15	88.15	93.48	92.52
	0.0001	50	93.33	87.63	91.63	86.96
		100	93.04	87.56	90.96	89.56
		200	93.7	89.85	92.96	90.15
R2	0.001	50	92.59	92.74	88.59	91.93
		100	94.07	87.33	89.85	86.81
		200	92.96	88.96	93.04	91.33
	0.0001	50	93.33	82.67	91.33	88
		100	92.89	86.59	91.56	91.56
		200	93.48	89.63	92.15	86.37
R3	0.001	50	96.59	99.04	97.48	97.85
		100	96.3	98.96	97.33	97.85
		200	96.52	98.89	97.7	98.52
	0.0001	50	95.85	98.07	96.81	96.67
		100	95.93	98.74	96.37	97.7
		200	96.44	99.11	97.04	98.59
ResNet50	0.001	50	94.00	86.74	92.52	92.30
		100	94.59	90.07	93.56	91.41
		200	94.22	88.89	94.07	92.22
	0.0001	50	93.33	88.52	92.74	92.67
		100	92.89	87.48	91.85	93.26
		200	93.70	89.19	92.15	91.85

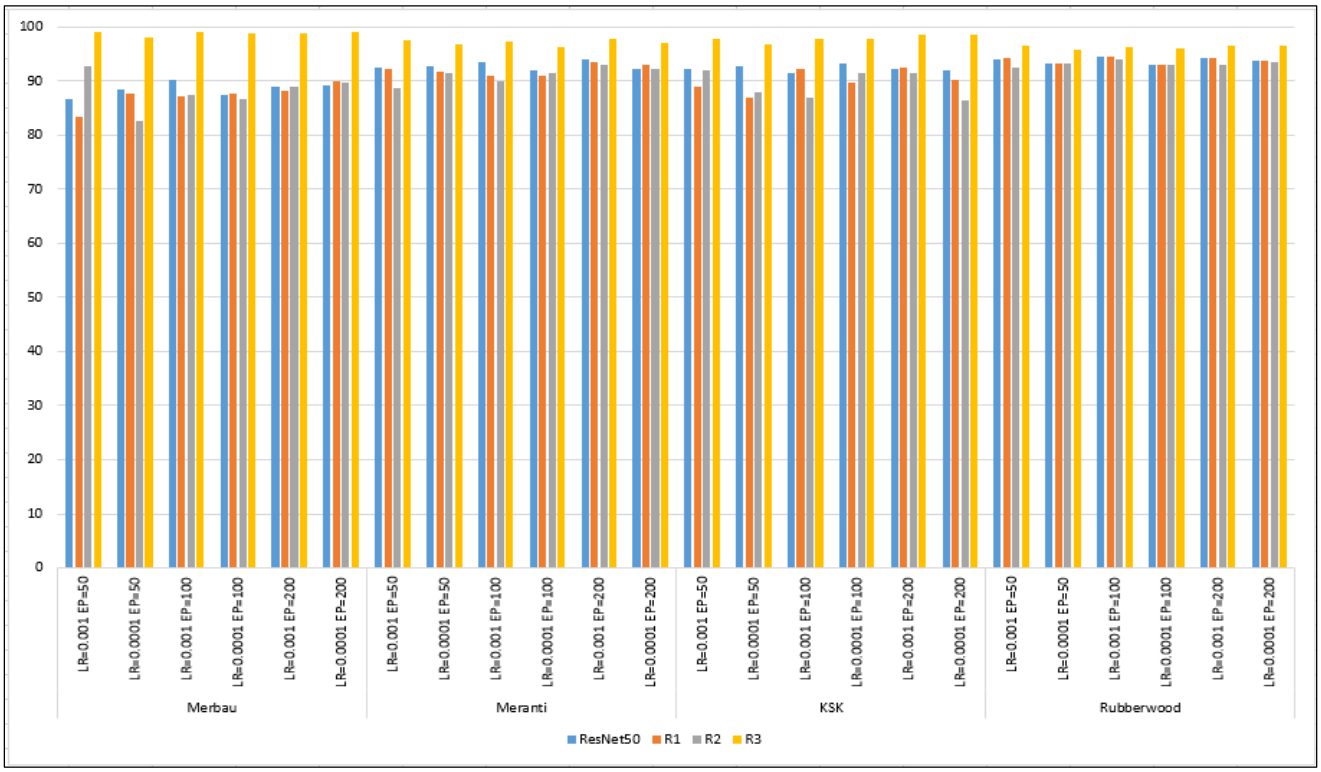

Fig. 4. Overall performance of proposed architectures and ResNet50.

To conduct further assessment, the classification performance of the R3 architecture was compared with ResNet50 and other proposed architectures using a one-way ANOVA test to identify any statistically significant differences in accuracy between the independent groups. The findings indicate that the classification performance of the proposed R3 architecture is statistically significantly superior compared to other architectures across multiple timber species. This implies the acceptance of the alternative hypothesis (HA) which indicate that there are at least two group means that are statistically significantly different from each other.

IV. Conclusion

This study presents an overview of the proposed timber defect identification framework based on the concept of residual neural network (ResNet) that mitigates the subjectivity and lack of precision associated with current timber defect identification methods, offering a more robust and reliable approach for the timber industry. It explores the evaluation of the approach concerning the number of stacked layers (depth) in the residual network architecture, as well as the integration of fully pre-activation activation functions within the residual block. Experiment are first conducted on the three proposed architectures (R1, R2, and R3) using various combinations of hyperparameters, including epochs and learning rates. The results from these experiments show that the R3 architecture which is formulated based on both stacked layers and fully pre-activation activation functions significantly contributes to satisfactory defect identification performance across all defect types and with consistently high accuracy observed across multiple timber species.

Acknowledgment

This research is supported by the Ministry of Higher Education (MOHE), Malaysia through Fundamental Research Grant Scheme (FRGS/1/2022/ICT02/UTEM/02/2) and Universiti Teknikal Malaysia Melaka.

References

[1] Y. Yang, X. Zhou, Y. Liu, Z. Hu, and F. Ding, “Wood defect detection based on depth extreme learning machine,” Appl. Sci., vol. 10, no. 21, p. 7488, 2020, doi: 10.3390/app10217488.

[2] J. Sandak, A. Sandak, A. Zitek, B. Hintestoisser, and G. Picchi, “Development of low-cost portable spectrometers for detection of wood defects,” Sensors, vol. 20, no. 2, p. 545, 2020, doi: 10.3390/s20020545.

[3] M. Kryl, L. Danys, R. Jaros, R. Martinek, P. Kodytek, and P. Bilik, “Wood recognition and quality imaging inspection systems,” J. Sensors, vol. 2020, 2020, doi: 10.1155/2020/3217126.

[4] R. N. N. Rahiddin, U. R. Hashim, L. Salahuddin, K. Kanchymalay, A. P. Wibawa, and T. H. Chun, “Local Texture Representation for Timber Defect Recognition based on Variation of LBP,” Int. J. Adv. Comput. Sci. Appl., vol. 13, no. 10, pp. 443–448, 2022, doi: 10.14569/IJACSA.2022.0131053.

[5] U. R. ah Hashim, S. Z. M. Hashim, A. K. Muda, K. Kanchymalay, I. E. A. Jalil, and M. H. Othman, “Single class classifier using FMCD based non-metric distance for timber defect detection,” Int. J. Adv. Soft Comput. its Appl., vol. 9, no. 3, pp. 199–216, 2017.

[6] H. S. Munawar, A. W. A. Hammad, A. Haddad, C. A. P. Soares, and S. T. Waller, “Image-based crack detection methods: A review,” Infrastructures, vol. 6, no. 8, pp. 1–20, 2021, doi: 10.3390/infrastructures6080115.

[7] K. Kamal, R. Qayyum, S. Mathavan, and T. Zafar, “Wood defects classification using laws texture energy measures and supervised learning approach,” Adv. Eng. Informatics, vol. 34, no. February, pp. 125–135, 2017, doi: 10.1016/j.aei.2017.09.007.

[8] K. Chaiyasarn, W. Khan, L. Ali, M. Sharma, D. Brackenbury, and M. DeJong, “Crack detection in masonry structures using convolutional

neural networks and support vector machines," in ISARC. Proceedings of the international symposium on automation and robotics in construction, 2018, vol. 35, pp. 1–8, doi: 10.22260/isarc2018/0016.

[9] U. R. Hashim et al., "Extraction and Exploratory Analysis of Texture Features on Images of Timber Defect," Adv. Sci. Lett., vol. 24, no. 2, pp. 1104–1108, 2018, doi: 10.1166/asl.2018.10696.

[10] W. Luo and L. Sun, "An improved binarization algorithm of wood image defect segmentation based on non-uniform background," J. For. Res., vol. 30, no. 4, pp. 1527–1533, 2019, doi: 10.1007/s11676-019-00925-w.

[11] H. C. Teo et al., "Identification of wood defect using pattern recognition technique," Int. J. Adv. Intell. Informatics, vol. 7, no. 2, pp. 163–176, Apr. 2021, doi: 10.26555/ijain.v7i2.588.

[12] G. Ramesh, T. Siddhartha, K. Sivaraman, and V. Subramani, "Identification of Timber Defects Using Convolution Neural Network," Proc. 6th Int. Conf. Commun. Electron. Syst. ICCES 2021, pp. 1641–1647, 2021, doi: 10.1109/ICCES51350.2021.9489136.

[13] J. Hu, W. Song, W. Zhang, Y. Zhao, and A. Yilmaz, "Deep learning for use in lumber classification tasks," Wood Sci. Technol., vol. 53, no. 2, pp. 505–517, 2019, doi: 10.1007/s00226-019-01086-z.

[14] N. D. Abdullah, U. R. Hashim, S. Ahmad, and L. Salahuddin, "Analysis of texture features for wood defect classification," Bull. Electr. Eng. Informatics, vol. 9, no. 1, pp. 121–128, 2020, doi: 10.11591/eei.v9i1.1553.

[15] T. He, Y. Liu, Y. Yu, Q. Zhao, and Z. Hu, "Application of deep convolutional neural network on feature extraction and detection of wood defects," Measurement, vol. 152, p. 107357, 2020, doi: 10.1016/j.measurement.2019.107357.

[16] F. Ding, Z. Zhuang, Y. Liu, D. Jiang, X. Yan, and Z. Wang, "Detecting defects on solid wood panels based on an improved SSD algorithm," Sensors, vol. 20, no. 18, pp. 1–17, 2020, doi: 10.3390/s20185315.

[17] A. Urbonas, V. Raudonis, R. Maskeliūnas, and R. Damaševičius, "Automated identification of wood veneer surface defects using faster region-based convolutional neural network with data augmentation and transfer learning," Appl. Sci., vol. 9, no. 22, p. 4898, 2019, doi: 10.3390/app9224898.

[18] Y. Huang, C. Qiu, X. Wang, S. Wang, and K. Yuan, "A compact convolutional neural network for surface defect inspection," Sensors (Switzerland), vol. 20, no. 7, pp. 1–19, 2020, doi: 10.3390/s20071974.

[19] A. Paulauskaite-Taraseviciene, K. Sutiene, and L. Pipiras, "Wooden dowels classification using convolutional neural network," Proc. Rom. Acad. Ser. A-Mathematics Phys. Tech. Sci. Inf. Sci., vol. 20, no. 4, pp. 401–408, 2019.

[20] M. Gao, J. Chen, H. Mu, and D. Qi, "A transfer residual neural network based on ResNet-34 for detection of wood knot defects," Forests, vol. 12, no. 2, p. 212, 2021, doi: 10.3390/f12020212.

[21] J. Liang, "Image classification based on RESNET," J. Phys. Conf. Ser., vol. 1634, no. 1, 2020, doi: 10.1088/1742-6596/1634/1/012110.

[22] K. He, X. Zhang, S. Ren, and J. Sun, "Deep residual learning for image recognition," in Proceedings of the IEEE conference on computer vision and pattern recognition, 2016, vol. 45, no. 8, pp. 770–778, doi: 10.1002/chin.200650130.

[23] R. K. Srivastava, K. Greff, and J. Schmidhuber, "Highway networks," arXiv Prepr. arXiv1505.00387, vol. 38, no. 11, pp. 1299–1316, Sep. 2015, [Online]. Available: http://arxiv.org/abs/1505.00387.

[24] I. Goodfellow, Y. Bengio, and A. Courville, Deep learning, vol. 13, no. 1. MIT press, 2016.

[25] A. S. Oktaria, E. Prakasa, and E. Suhartono, "Wood Species Identification using Convolutional Neural Network (CNN) Architectures on Macroscopic Images," J. Inf. Technol. Comput. Sci., vol. 4, no. 3, pp. 274–283, 2019, doi: 10.25126/jitecs.201943155.

[26] I. Z. Mukti and D. Biswas, "Transfer learning based plant diseases detection using ResNet50," in 2019 4th International Conference on Electrical Information and Communication Technology (EICT), 2019, pp. 1–6.

[27] C. F. Ahmed, A. Cheema, W. Qayyum, and R. Ehtisham, "Detection of Pavement cracks of UET Taxila using pre-trained model Resnet50 of Detection of Pavement cracks of UET Taxila using pre-trained model Resnet50 of CNN," Proc. 1st Int. Conf. Adv. Civ. Environ. Eng. Taxila Pakistan, no. March, pp. 5–6, 2022.

[28] A. Krizhevsky, I. Sutskever, and G. E. Hinton, "Imagenet classification with deep convolutional neural networks," Commun. ACM, vol. 60, no. 6, pp. 84–90, 2017, doi: 10.1145/3065386.

[29] H. C. Teo, U. R. Hashim, S. Ahmad, L. Salahuddin, N. H. Choon, and K. Kanchymalay, "Efficacy of the Image Augmentation Method using CNN Transfer Learning in Identification of Timber Defect," Int. J. Adv. Comput. Sci. Appl., vol. 13, no. 5, pp. 107–115, 2022, doi: 10.14569/ijacsa.2022.0130514.

[30] H. C. Teo et al., "A review of the automated timber defect identification approach," Int. J. Electr. Comput. Eng., vol. 13, no. 2, pp. 2156–2166, 2023, doi: 10.11591/ijece.v13i2.pp2156-2166.

[31] R. Ehtisham, W. Qayyum, C. V Camp, J. Mir, and A. Ahmad, "Predicting the defects in wooden structures by using pre-trained models of Convolutional Neural Network and Image Processing," in 2nd International Conference on Recent Advances in Civil Engineering and Disaster Management, 2022, pp. 208–212.

[32] B. Zoph, V. Vasudevan, J. Shlens, and Q. V. Le, "Learning transferable architectures for scalable image recognition," in Proceedings of the IEEE conference on computer vision and pattern recognition, 2018, pp. 8697–8710, doi: 10.1109/CVPR.2018.00907.

[33] R. Ehtisham et al., "Classification of defects in wooden structures using pre-trained models of convolutional neural network," Case Stud. Constr. Mater., vol. 19, no. September, p. e02530, 2023, doi: 10.1016/j.cscm.2023.e02530.

[34] D. Theckedath and R. R. Sedamkar, "Detecting affect states using VGG16, ResNet50 and SE-ResNet50 networks," SN Comput. Sci., vol. 1, no. 2, p. 79, 2020, doi: 10.1007/s42979-020-0114-9.

[35] K. He, X. Zhang, S. Ren, and J. Sun, "Identity mappings in deep residual networks," Lect. Notes Comput. Sci. (including Subser. Lect. Notes Artif. Intell. Lect. Notes Bioinformatics), vol. 9908 LNCS, pp. 630–645, 2016, doi: 10.1007/978-3-319-46493-0_38.

[36] U. R. Hashim, S. Z. Hashim, and A. K. Muda, "Image collection for non-segmenting approach of timber surface defect detection," Int. J. Adv. Soft Comput. its Appl., vol. 7, no. 1, pp. 15–34, 2015.